A water-promoted Mars-van-Krevelen reaction dominates low-temperature CO oxidation over Au-Fe_2O_3, but not over Au-TiO_2

Alexander Holm,[‡] Bernadette Davies,[‡] Sara Boscolo Bibi, Felix Santiago Moncada Arias, Joakim Halldin-Stenlid, Laurynas Paškevičius, Vincent Claman, Adam Slabon, Cheuk-Wai Tai, Egon Campos dos-Santos, Sergey Koroidov[*]

[‡] *These authors contributed equally to this work*

**Corresponding author:*
Sergey Koroidov
Department of Physics, Stockholm University
E-mail: sergey.koroidov@fysik.su.se

ABSTRACT: We provide experimental evidence that is inconsistent with often proposed Langmuir-Hinshelwood (LH) mechanistic hypotheses for water-promoted CO oxidation over Au-Fe_2O_3. Passing CO and H_2O, but no O_2, over Au-γ-Fe_2O_3 at 25°C, we observe significant CO_2 production, inconsistent with LH mechanistic hypotheses. Experiments with $H_2{}^{18}O$ further show that previous LH mechanistic proposals cannot account for water-promoted CO oxidation over Au-γ-Fe_2O_3. Guided by density functional theory, we instead postulate a water-promoted Mars-van-Krevelen (w-MvK) reaction. Our proposed w-MvK mechanism is consistent both with observed CO_2 production in absence of O_2, and with CO oxidation in presence of $H_2{}^{18}O$ and $^{16}O_2$. In contrast, for Au-TiO_2, our data is consistent with previous LH mechanistic hypotheses.

KEYWORDS: CO oxidation, Mars-van-Krevelen, Langmuir-Hinshelwood, mechanism, Au, Fe_2O_3, TiO_2

CO oxidation over Au nanoparticles (NPs) on metal oxides is intensely studied in heterogeneous catalysis.[1–22] Water strongly promotes this reaction, making catalysts up to one order of magnitude more active at room-temperature.[10,12–15,17,20,23] However, there is still much debate regarding the mechanism behind water-promotion. At the center of this debate is whether support lattice-oxygen takes an active

part in the reaction (a Mars van Krevelen mechanism, MvK) or if the reaction takes place exclusively between co-adsorbed reaction intermediates (a Langmuir-Hinshelwood mechanism, LH).

With support from theory,[1,19] spectroscopy,[3,5,6,24,25] temporal analysis of products,[9,10] and isotope exchange experiments,[5,26] it has been argued that room-temperature CO oxidation occurs via a lattice-mediated Mars-van-Krevelen reaction over Au-TiO_2 and Au-Fe_2O_3. However, as pointed out by Chandler,[12] current mechanistic proposals involving the support lattice do not clearly account for water-promotion. In contrast, various LH-mechanisms have been proposed that could account for this promotion.[12–18] In particular, two influential studies have proposed that a LH-type mechanism can rationalize water-promotion on both non-reducible (e.g., Al_2O_3) and reducible (e.g., TiO_2, Fe_2O_3) supports.[12,13] Chandler et al. observed that, at room-temperature, CO and O_2 rate orders, kinetic isotope (hydrogen / deuterium) effects and H_2O adsorption were similar over Au-Al_2O_3 and Au-TiO_2, implying that the catalysts run by the same mechanism. It was argued that because lattice-oxygen on non-reducible Al_2O_3 cannot directly participate in the reaction mechanism, and because the data implied that Au-Al_2O_3 and Au-TiO_2 operate by the same mechanism, lattice-oxygen does not participate in room-temperature water-promoted CO oxidation over Au-TiO_2. Chandler therefore proposed that water-promotion over Au-TiO_2 and Au-Al_2O_3 occurs by a LH-mechanism with CO adsorbing on Au NPs, and H_2O adsorbing on the Au-support interface, there promoting O_2 activation to form a reactive hydroperoxy species (OOH) which then reacts with adsorbed

Scheme 1. Elementary reaction steps for the (by Chandler et al.) [12] postulated LH-reaction mechanism of water-promoted CO oxidation over Au-Al_2O_3 and Au-TiO_2 which has also been proposed[15] to be dominant on Au-Fe_2O_3. Note: * denotes an active site on the Au NP, away from the NP-support interface, † denotes an Au site at the NP-support interface, and ‡ denotes a support site at the NP-support interface. Formal charges that form during the reaction are assumed to be balanced by formal charges distributed over the Au NP.[12]

R1.	2 x (CO (g) + * → *CO)
R2.	2 x (H_2O (g) + ‡ → H_2O‡)
R3.	H_2O‡ + O_2 (g) + † → †OOH + ‡OH^-
R4.	†OOH + *CO → *COOH + O†
R5.	*COOH + H_2O‡ → * + CO_2 (g) + H_3O^+ ‡
R6.	O† + *CO → † + * + CO_2 (g)
R7.	‡OH^- + H_3O^+ ‡ → 2 H_2O (g) + 2 ‡
Σ	2 CO (g) + O_2 → 2 CO_2 (g)

Scheme 2. Elementary reaction steps for a previously (by Iglesia et al.)[13] postulated LH-reaction mechanism of water-promoted CO oxidation over Au-Al_2O_3, Au-TiO_2, and Au-Fe_2O_3. Note: * denotes an active site on the Au NP.

R8.	2 x (CO (g) + * → *CO)
R9.	O_2 (g) + * → *O_2
R10.	H_2O (g) + * → H_2O*
R11.	*O_2 + H_2O* → *OOH + *OH
R12.	*OOH + *CO → *OH + CO_2 (g) + *
R13.	*OH + *OH → H_2O (g) + O*
R14.	*CO + O* → CO_2 (g) + 2*
Σ	2 CO (g) + O_2 → 2 CO_2 (g)

CO to form CO_2 (Scheme 1).[12] In this reaction scheme, no oxygen from water would be incorporated into CO_2, as the water-promotion occurs through a series of proton transfers only. Recently, the LH-mechanism proposed by Chandler for Au-TiO_2 and Au-Al_2O_3 was also proposed to account for water-promotion over Au-Fe_2O_3.[15]

Before Chandler, Iglesia et al. postulated a related LH-mechanism for water-promoted CO oxidation over Au-Al_2O_3, Au-TiO_2 and Au-Fe_2O_3 (Scheme 2). Similar to Chandler, it was hypothesized that only adsorbed intermediates participate in the reaction, and that water-promotion occurs because water activates O_2 to form OOH (Scheme 2). Observing that the rate equations derived from this mechanism accurately predicted rate orders and rates over all catalysts (Au-Al_2O_3, Au-TiO_2 and Au-Fe_2O_3), the authors proposed that this LH-mechanism was dominant over the catalysts.[13]

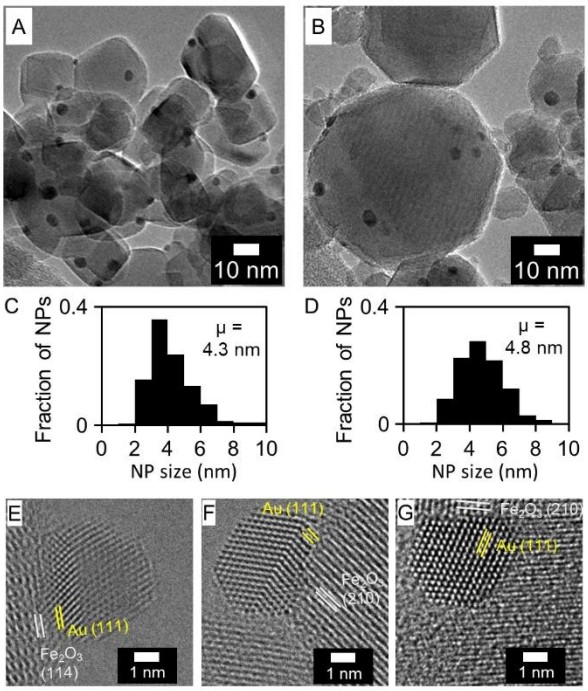

Figure 1. (A) TEM micrograph of Au-TiO_2, and **(B)** of Au-γ-Fe_2O_3. **(C)** Au NP size histogram for Au-TiO_2 and **(D)** for Au-γ-Fe_2O_3. **(E) – (G)** Typical high resolution TEM images of Au-γ-Fe_2O_3. The Au NPs are polyhedral, with the (111) facet dominating at the Au/γ-Fe_2O_3 interface. For γ-Fe_2O_3, many facets are present, e.g., (114) and (210).

Here we provide experimental data clearly demonstrating that a LH-type mechanism cannot dominate water-promoted CO oxidation over Au-γ-Fe_2O_3 at room-temperature. Instead, we postulate that a lattice-mediated mechanism, which do account for water-promotion, dominates. We present DFT calculations and careful CO oxidation experiments with $C^{16}O$, $^{16}O_2$, and $H_2{}^{18}O$ suggesting that this mechanism can rationalize water-promoted CO oxidation over Au-γ-Fe_2O_3.

We prepared Au-TiO_2 and Au-γ-Fe_2O_3 catalysts by well-established protocols (Supporting Information, Section S1), resulting in Au NP sizes of 4.3 nm (Au-TiO_2) and 4.8 nm (Au-γ-Fe_2O_3), similar to previous reports (Figure 1 A - D).[13,21,27–30] The Au-γ-Fe_2O_3 catalyst was characterized in more detail, and consists of polyhedral Au NPs supported on γ-Fe_2O_3, where the Au(111) facet is dominating at the Au/γ-Fe_2O_3 perimeter, while many γ-Fe_2O_3 facets are present, e.g., (114) and (210), Figure 1 E - G.

Investigation by high-resolution STEM (Supporting Figure S10) found no evidence of single Au atoms, suggesting that Au NPs are the dominant Au species in the catalyst.

Catalytic tests were run at ambient temperature (controlled at 25 ^{o}C), consistent with previous studies.[3,5,6,12–15,21,28,29,31–34] Ambient oxygen adsorbed to the catalyst was removed by passing humidified N_2 (2.8 vol % H_2O) over the catalyst for 16 h. We then introduced CO (1 vol %) in the inlet flow. Over Au-TiO_2, no significant CO_2 production was observed (Figure 2 A), while over Au-γ-Fe_2O_3, CO_2 production quickly increased to 0.95 mmol CO_2 (mol Au)$^{-1}$ s^{-1}, then rapidly decreasing (Figure 2 B). The background O_2 concentration in our reactor is ≈ 4 ppm, which is about 2 % of the CO_2 concentration resulting from CO oxidation (Supporting Figure S5 and Figure S6). In addition, no H_2 is produced (Supporting Figure S7), ruling out the possibility that the water gas shift reaction (CO + H_2O → CO_2 + H_2), contributes to CO_2 production. Thus, over Au-γ-Fe_2O_3, water-promoted CO oxidation in the absence of O_2 occur with removal of oxygen from the γ-Fe_2O_3 lattice. Of course, the CO_2 production in the absence of O_2 is not stable because the γ-Fe_2O_3 lattice is gradually depleted of oxygen.

Thus, water-promoted CO oxidation over Au-γ-Fe_2O_3 can proceed by abstraction of lattice-oxygen, while over Au-TiO_2, this appears unlikely. Our data, therefore does not refute previously

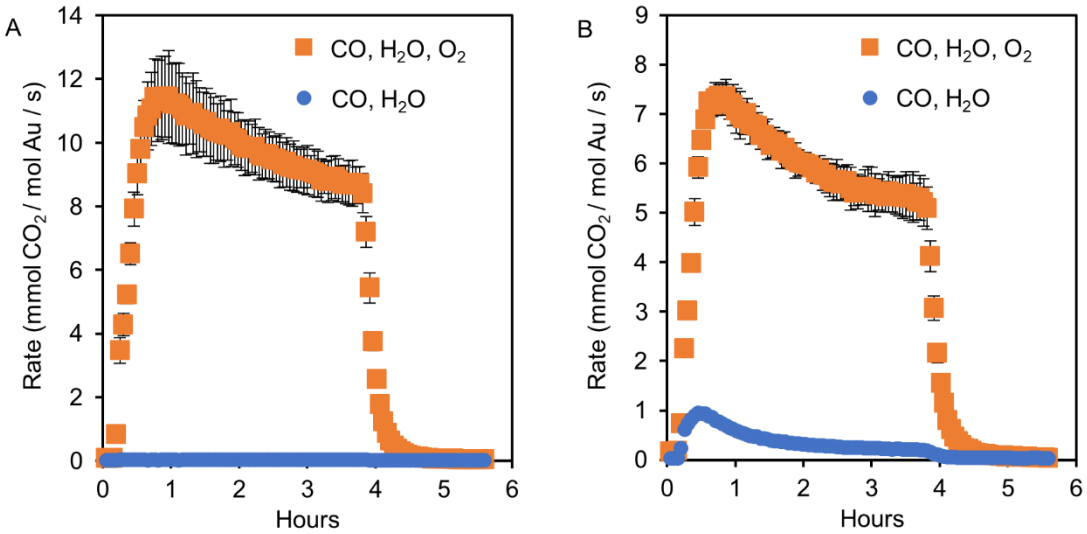

Figure 2. (A) Transient CO oxidation rates over Au-TiO_2. **(B)** Transient CO oxidation rates over Au-γ-Fe_2O_3. Reaction starts immediately upon introduction of CO, and terminates immediately upon removal of CO (at 3 h 45 min). Orange squares: 1 vol % CO, 2.8 vol % H_2O, 20 vol % O_2, balance N_2. Blue circles: 1 vol % CO, 2.8 vol % H_2O, balance N_2. Reaction temperature was 25 ^{o}C, and pressure 1 atm. The gas hourly space velocity (GHSV) was 21 L h^{-1} g$^{-1}_{cat}$, and the CO conversion was below 20 % (ensuring data was collected under differential conditions).[13,37] Reported curves are averages of three independent measurements. Error bars are 2 standard deviations wide. For some data points, the error-bars are so small, they are obscured by the data-labels. Full data-sets in Supporting Figure S8.

proposed LH mechanisms over Au-TiO_2. However, over Au-γ-Fe_2O_3, we need to investigate how significant the lattice reaction is when O_2 is present. To probe this question, we assessed water-promoted CO oxidation with O_2, for both Au-TiO_2 (Figure 2 A) and Au-Fe_2O_3 (Figure 2 B). The rates measured are similar[a] to previously reported rates,[3,5,6,21,28,29,31–34] showing that our catalysts are comparable to previously reported catalysts. Over Au-γ-Fe_2O_3, the maximum rate in the presence of water, but without O_2 (0.95 mmol CO_2 (mol Au)$^{-1}$ s^{-1}) is ≈ 13 % of the maximum rate with O_2. This suggests that a lower bound of ≈ 13 % CO_2 is produced by a water-promoted lattice-route during CO oxidation over Au-γ-Fe_2O_3. However, the true contribution is likely higher, since with O_2 present, lattice-oxygen is continuously replenished. Below, we further investigate what this true contribution may be, using a combination of DFT computation and CO oxidation experiments in the presence of $H_2{}^{18}O$.

Scheme 3. Elementary reaction steps for our proposed water-promoted w-MvK CO oxidation mechanism (R15, R17 - R21). The (non-feasible) non-water promoted MvK mechanism is represented by R15, R16, R20, R21. Note: * denotes an active site on the Au NP, O_{lat} denotes a lattice-oxygen, near the Au NP, $\square_{O_{lat}}$ denotes a lattice-oxygen vacancy, OH_{ad} denotes a hydroxyl on a lattice-Fe, OH_{lat} denotes a hydroxyl in a lattice oxygen position.

R15.	2 x (CO (g) + * → *CO)
R16.	*CO + O_{lat} → CO_2 + * + $\square_{O_{lat}}$
R17.	H_2O (g) + O_{lat} → OH_{ad} + OH_{lat}
R18.	*CO + OH_{ad} → *COOH
R19.	*COOH + OH_{lat} → CO_2 (g) + H_2O (g) + * + $\square_{O_{lat}}$
R20.	O_2 (g) + $\square_{O_{lat}}$ + * → O_{lat} + O*
R21.	O* + *CO → CO_2 (g) + 2 *
Σ (w-MvK, MvK)	2 CO (g) + O_2 → 2 CO_2 (g)

To rationalize the observed CO_2 production over Au-γ-Fe_2O_3 in the absence of O_2, a lattice reaction (MvK) mechanism must be invoked. Considering the exposed Au and γ-Fe_2O_3 facets (Figure 1 E – G), a suitable Au-γ-Fe_2O_3 model system was created (Supporting Information, Section S2), using density functional theory (DFT). Using this system, we found a low barrier, water-promoted MvK (w-MvK) mechanism, presented in Scheme 3 and Figure 3. A similar mechanism has been proposed for water-promoted CO oxidation over single-atom Pt_1-CeO_2,[35] and we propose that this mechanism can be adapted to rationalize room-temperature CO oxidation over Au-γ-Fe_2O_3.

Direct abstraction of γ-Fe_2O_3 lattice-oxygen by Au-adsorbed CO comes with a prohibitively high barrier of 0.98 eV (reaction R16). However, introduction of water presents a low-barrier alternative (to R16), but likewise lattice-mediated, path for CO oxidation (R17 – R19, scheme 3). Reaction R17 describes

[a] Rates should be compared after normalizing by the total Au-NP / support interface perimeter in the different studies. It has been shown that CO oxidation activity for Au-Fe_2O_3 and Au-TiO_2 is proportional to this perimeter.[5]

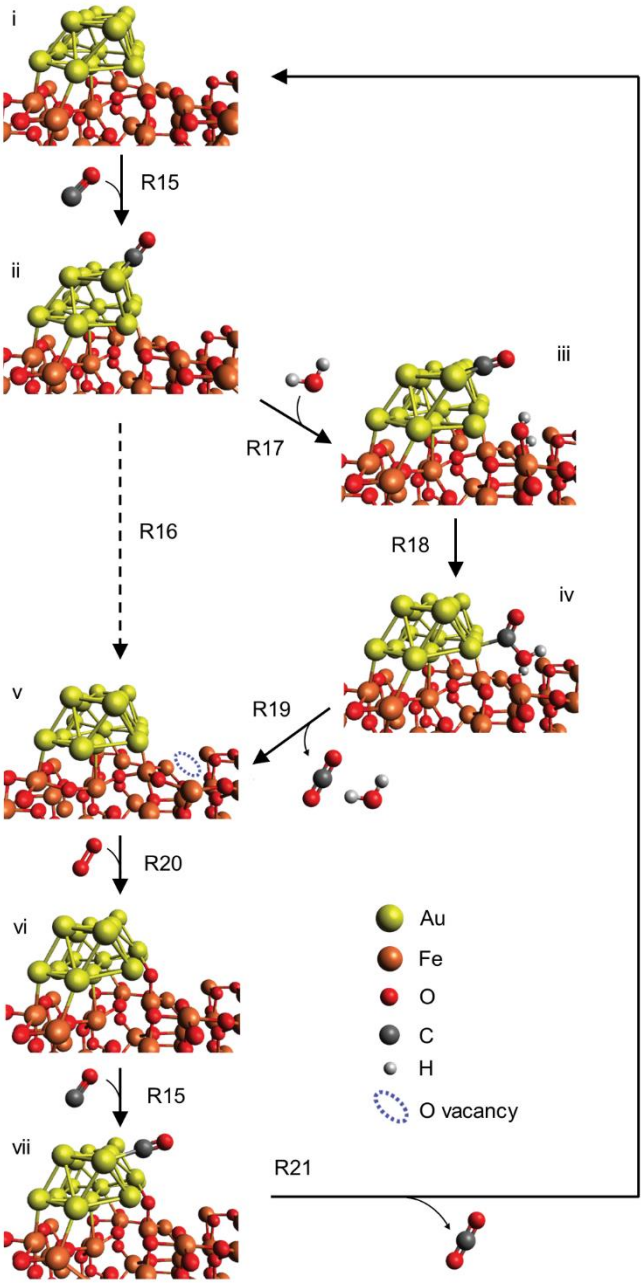

Figure 3. Schematic representation of our proposed mechanism for w-MvK CO oxidation (R15, R17 – R21) over Au-γ-Fe_2O_3. The non-feasible, non-water promoted, MvK mechanism is represented by R15, R16, R20, R21.

dissociative adsorption of H_2O onto an Fe_{lat}-O_{lat} motif in the γ-Fe_2O_3 surface, with H_2O splitting into a hydroxyl on top of Fe_{lat} (OH_{ad}) and a lattice-hydroxyl (OH_{lat}) (Figure 3). Reaction R18 describes the reaction of CO, adsorbed on gold, with the water-derived OH_{ad} to form a carboxylic group (COOH) adsorbed to the Au NP. This carboxylic group then reacts (R19) with the OH_{lat} formed during water dissociation (R17) to produce CO_2 and re-form H_2O, thereby forming a lattice oxygen vacancy. Note from reactions R17 – R19 that water is first consumed, and then re-generated, such that no net-consumption of water occurs, and water acts purely as a promoter. Also note that, although oxygen from water is incorporated into CO_2, water is regenerated with oxygen from the γ-Fe_2O_3 lattice, meaning that overall, reactions R17 – R19 yields the same stoichiometry as reaction R16 (Scheme 3 and Figure 3). The critical point is that the water-mediated abstraction of lattice-oxygen (in the form of OH_{lat}) is energetically more favorable than O_{lat} abstraction in the absence of water. Between reactions R17 – R19, reaction R18 has the highest barrier (0.44 eV), to compare with the barrier for direct abstraction of O_{lat} by CO (R16, 0.98 eV). Reaction R20 describes the filling of an oxygen vacancy with oxygen from O_2 (g), forming an oxygen atom (O*) on the Au NP in the process. The catalytic cycle closes (R21) with Au-adsorbed CO reacting with this oxygen atom to form CO_2. These final steps (R20, R21) of the catalytic cycle are essentially without barriers (Figure 4).

To compare our proposed w-MvK mechanism (Scheme 3) with previously proposed LH-mechanisms (Scheme 1 and Scheme 2), we also calculated the reaction barriers for these LH mechanisms (Figure 4). We calculated activation energies for the LH mechanisms proposed by Chandler (Scheme 1) and Iglesia (Scheme 2), and find that they share the rate determining step, namely O_2 (g) activation by water to form OOH. We calculate the activation energy for this step (R3 in Chandler's mechanism, and R11 in Iglesia's mechanism) to 0.55 eV (Supporting Information, Table S2). Our calculations therefore indicate that the w-MvK mechanism may be favored over these previously proposed LH mechanisms. However, the similar reaction barriers suggests that an LH mechanism and a MvK mechanism potentially could operate simultaneously over Au- γ-Fe_2O_3 (although, as shown above, a lower bound of 13 % CO_2 must result from a MvK mechanism). To further distinguish between the mechanisms, we turned to experiments of $H_2{}^{18}O$ - promoted CO oxidation.

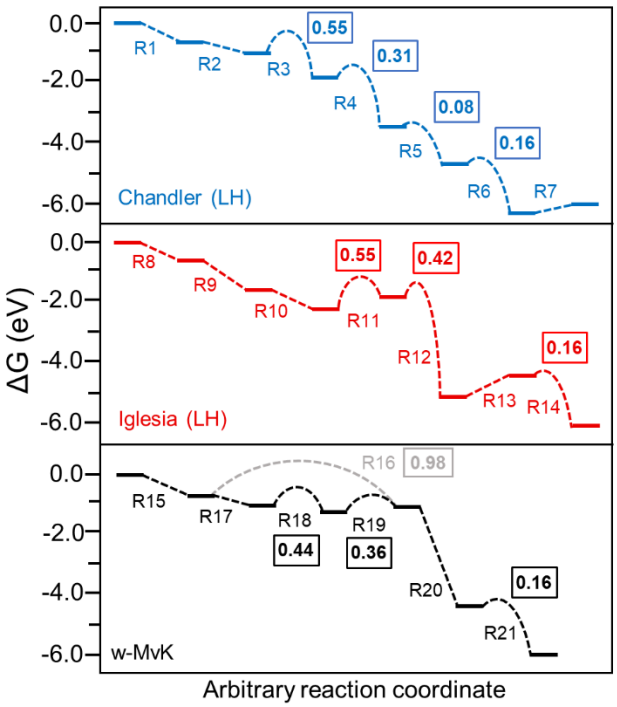

Figure 4. Energy diagrams of previously proposed LH mechanisms and of our proposed w-MvK mechanism. The reactions are labelled according to Schemes 1 – 3. Boxed values (in eV) are activation energies for the respective elementary reaction.

Different mechanisms of $H_2{}^{18}O$ - promoted $C^{16}O$ oxidation would lead to different abundances of $C^{16}O_2$, ($C^{18}O^{16}O$ + $C^{16}O^{18}O$), and $C^{18}O_2$. Chandler's mechanism would lead to no ^{18}O incorporation into CO_2 (100 % $C^{16}O_2$ expected). In contrast, Iglesia's mechanism would lead to 75 % $C^{16}O_2$, and 25 % ($C^{18}O^{16}O$ + $C^{16}O^{18}O$), while our proposed w-MvK mechanism should result in relative abundancies of 50 % $C^{16}O_2$ and 50 % ($C^{18}O^{16}O$ + $C^{16}O^{18}O$). Please refer to the Supporting Information, Section S4, for a detailed analysis of how these relative isotopic CO_2 abundancies can be predicted from the respective mechanisms.

Before we discuss the experimentally observed relative abundancies, we note that CO_2 also exchanges oxygen directly with $H_2{}^{18}O$.[36] This exchange occurs in the reactor piping and on the catalyst bed, and is therefore a reactor-specific property that must be deconvoluted from the abundancies resulting

from ^{18}O insertion into CO_2 due to the CO oxidation mechanism. To estimate the ^{18}O exchange between $H_2{}^{18}O$ and different isotopic CO_2 species in our reactor, we prepared a mixture of $C^{16}O_2$, $H_2{}^{18}O$ and $^{16}O_2$ with the same concentrations as obtained during CO oxidation. We then passed this mixture over the Au-γ-Fe_2O_3 catalyst, at the same conditions used for $C^{16}O$ oxidation. This experiment allowed us to deduce (Supporting Information, Section S4) the reactor-specific probabilities that a given CO_2 species ($C^{16}O^{16}O$, $C^{18}O^{16}O$, $C^{16}O^{18}O$ or $C^{18}O^{18}O$) transforms to another isotopic CO_2 species by ^{18}O exchange with $H_2{}^{18}O$:

$$P_{exch.}(C^{16}O^{16}O \rightarrow C^{18}O^{16}O) = P_{exch.}(C^{16}O^{16}O \rightarrow C^{16}O^{18}O) = 0.18 \quad (1)$$

$$P_{exch.}(C^{16}O^{16}O \rightarrow C^{18}O^{18}O) = 0.07 \quad (2)$$

$$P_{exch.}(C^{18}O^{16}O \rightarrow C^{18}O^{18}O) = P_{exch.}(C^{16}O^{18}O \rightarrow C^{18}O^{18}O) = 0.25 \quad (3)$$

With knowledge of our reactor-specific ^{18}O incorporation into different CO_2 species by exchange with $H_2{}^{18}O$, and with the abundancies predicted to result from the different CO oxidation mechanisms, we can now predict, for each hypothetical mechanism, the expected abundancies in the reactor effluent. For Iglesia's LH-mechanism (Scheme 2), we would expect 43 % $C^{16}O_2$, 46 % ($C^{18}O^{16}O$ + $C^{16}O^{18}O$), and 11 % $C^{18}O_2$. For Chandler's LH-mechanism (Scheme 1), we would expect 58 % $C^{16}O_2$, 36 % ($C^{18}O^{16}O$ + $C^{16}O^{18}O$), and 7 % $C^{18}O_2$. And finally, for our proposed w-MvK mechanism, we would expect 29 % $C^{16}O_2$, 56 % ($C^{18}O^{16}O$ + $C^{16}O^{18}O$), and 16 % $C^{18}O_2$. Please refer to the Supporting Information, Section S4, for detailed calculation of these predicted abundancies in the reactor effluent.

Transient CO oxidation experiments over Au-γ-Fe_2O_3, using $C^{16}O$, $^{16}O_2$ and $H_2{}^{18}O$ were then carried out (Figure 5) using the conditions described in Figure 2 (although GHSV was reduced, through the flow-rate, to allow prolonged bubbling through a small volume of $H_2{}^{18}O$). During CO oxidation, we measured transient production rates (Figure 5 A) of $C^{16}O_2$, ($C^{18}O^{16}O$ + $C^{16}O^{18}O$), and $C^{18}O_2$, then calculating their transient relative abundancies in the reactor effluent (Figure 5 B). The experimental abundancies thus found were 28 % $C^{16}O_2$, 55 % ($C^{18}O^{16}O$ + $C^{16}O^{18}O$), and 17 % $C^{18}O_2$ (Figure 5 C). It is note-worthy that, although the catalyst deactivates during reaction, the relative isotopic abundancies remain constant, suggesting that the same mechanism is dominant during the entire course of reaction.

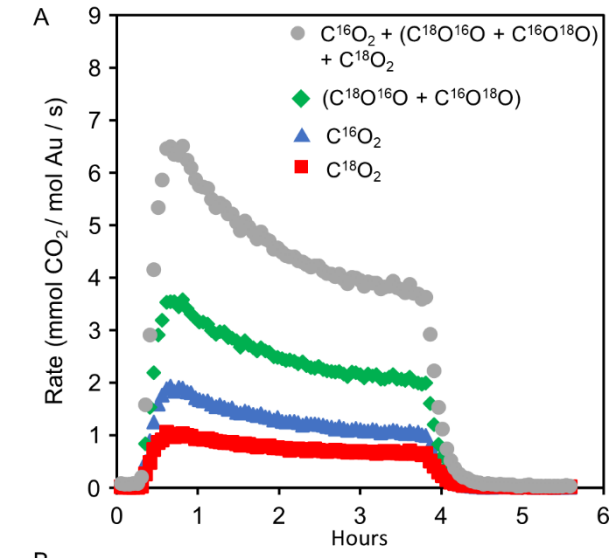

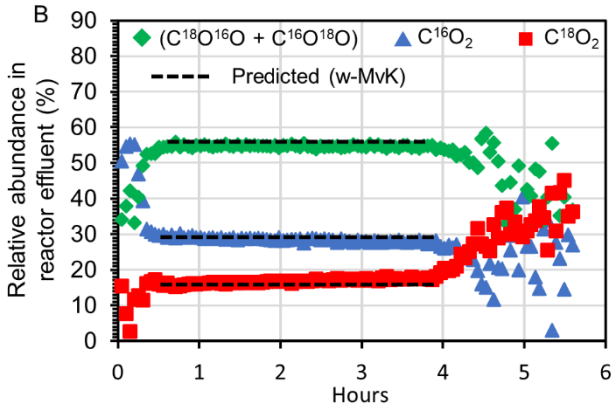

C

	Predicted and experimental relative abundancies in reactor effluent (%)		
	$C^{16}O_2$	($C^{18}O^{16}O$ + $C^{16}O^{18}O$)	$C^{18}O_2$
Chandler (LH)	58 %	36 %	7 %
Iglesia (LH)	43 %	46 %	11 %
w-MvK	29 %	56 %	16 %
Experimental	28 %	55 %	17 %

Figure 5. $C^{16}O$ oxidation over Au-γ-Fe_2O_3 with $H_2{}^{18}O$ and $^{16}O_2$. **(A)** Transient production rates of different isotopic CO_2 – species, and the total rate. **(B)** Transient relative abundancies of different isotopic CO_2 – species in the reactor effluent. Relative abundancies were calculated (e.g., for $C^{16}O_2$) as:

$$\frac{rate(C^{16}O_2)}{rate(C^{16}O_2) + rate(C^{18}O^{16}O + C^{16}O^{18}O) + rate(C^{18}O_2)} * 100$$

The relative abundancies predicted from our proposed w-MvK mechanism are indicated by dashed lines.
(C) Comparison between predicted (from different mechanistic hypotheses), and experimentally observed relative abundancies in the reactor effluent. Reaction conditions: 1 vol % $C^{16}O$, 2.8 vol % $H_2{}^{18}O$, 20 vol % $^{16}O_2$, balance N_2. Reaction temperature was 25°C, pressure 1 atm, and the space velocity (GHSV) was 10.5 L h^{-1} g^{-1}cat.

Comparing (Figure 5 C) the measured isotopic CO_2 abundancies during reaction with the abundancies predicted by the previously proposed LH mechanisms (Scheme 1 and Scheme 2), it is clear that these mechanisms are not consistent with the observed abundancies in the reactor effluent. In contrast, our proposed w-MvK mechanism predicts the observed isotopic CO_2 abundancies to within one percentage point (Figure 5 C). Put differently, the observed isotopic CO_2 abundancies — after correcting for ^{18}O exchange between CO_2 and $H_2{}^{18}O$ — suggests that $H_2{}^{18}O$ - promoted CO oxidation over Au-γ-Fe_2O_3 results in 50 % $C^{16}O_2$ and 50 % ($C^{18}O^{16}O$ + $C^{16}O^{18}O$). This is clearly inconsistent with previous LH-mechanisms, but is consistent with our proposed w-MvK mechanism.

In conclusion, since no significant lattice reaction is observed during water-promoted CO oxidation over Au-TiO_2, previously proposed LH-mechanisms[12–14,17,18] remain plausible for this system, at least at room-temperature. However, for water-promoted CO oxidation over Au-γ-Fe_2O_3, there is a lattice reaction that significantly contributes activity (Figure 2 B). By accounting for ^{18}O exchange between CO_2 and $H_2{}^{18}O$ in $H_2{}^{18}O$ - promoted CO oxidation, we find that the reaction mechanism leads to

isotopic abundancies of 50 % $C^{16}O_2$ and 50 % ($C^{18}O^{16}O$ + $C^{16}O^{18}O$). Taken together, these results specifically refute (at least for Au-γ-Fe_2O_3) two previously proposed LH mechanistic hypotheses[12,13] (Scheme 1 and Scheme 2), and also cast doubt over other[15,22,37,38] previous LH mechanistic proposals. In contrast, our proposed w-MvK mechanism (Scheme 3 and Figure 3) is consistent with the data, and constitute a useful mechanistic hypothesis.

While we have shown that our w-MvK mechanism can rationalize water-promoted CO oxidation over Au-γ-Fe_2O_3, we also believe that this mechanism can rationalize CO oxidation in nominally dry conditions. In catalytic tests at room-temperature, nominally dry gas streams will contain 1 – 10 ppm H_2O,[39] which — because water is not consumed — likely is sufficient for water-promotion.[13,17,23,39] Furthermore, our DFT calculations indicate that CO abstraction of lattice oxygen in absence of water is implausible (R16, 0.98 eV) compared to the water-promoted abstraction (R15, R17 – R21) with a barrier in the rate determining step of 0.44 eV. We therefore believe our w-MvK mechanism could rationalize observations[3,4,6] of a lattice reaction in nominally water-free CO oxidation over Au-γ-Fe_2O_3. Finally, because many studies show that a lattice reaction occurs also on Au-α-Fe_2O_3[3–6,10,27,40] we believe our proposed mechanism may operate also in these systems. We therefore believe our proposed w-MvK mechanism can rationalize CO oxidation over most Au-Fe_2O_3 catalysts in both nominally dry and in humid conditions.

Author Contributions A.H. and S.K. conceptualized the research. A.H., B.D., L.P.,V.C., C.W.T. and S.K. carried out experiments and characterization. E.D.S carried out the DFT study. A.H. wrote the original draft of the manuscript. All authors contributed to reviewing and editing of the manuscript. S.K. supervised the research.

ASSOCIATED CONTENT

Supporting Information. Section S1. Experimental details. Section S2. Computational details and results. Section S3. Miscellaneous Figures. Section S4. Calculation of predicted abundances of $C^{16}O_2$, ($C^{18}O^{16}O$ + $C^{16}O^{18}O$) and $C^{18}O_2$ resulting from $C^{16}O$ oxidation with $^{16}O_2$ and $H_2{}^{18}O$ over Au-γ-Fe_2O_3.

REFERENCES

(1) Duan, Z.; Henkelman, G. CO Oxidation at the Au/TiO2 Boundary: The Role of the Au/Ti5c Site. *ACS Catal* **2015**, *5* (3), 1589–1595. https://doi.org/10.1021/cs501610a.

(2) Wang, Y.; Cantu, D. C.; Lee, M.; Li, J.; Rousseau, R. CO Oxidation on Au / TiO 2 : Condition- Dependent Active Sites and Mechanistic Pathways. 1–17.

(3) Šmit, G.; Strukan, N.; Crajé, M. W. J.; Lázár, K. A Comparative Study of CO Adsorption and Oxidation on Au/Fe2O3 Catalysts by FT-IR and in Situ DRIFTS Spectroscopies. *J Mol Catal A Chem* **2006**, *252* (1–2), 163–170. https://doi.org/10.1016/j.molcata.2006.02.058.

(4) Šmit, G.; Zrnčević, S.; Lázár, K. Adsorption and Low-Temperature Oxidation of CO over Iron Oxides. *J Mol Catal A Chem* **2006**, *252* (1–2), 103–106. https://doi.org/10.1016/j.molcata.2006.02.051.

(5) Wei, X.; Shao, B.; Zhou, Y.; Li, Y.; Jin, C.; Liu, J.; Shen, W. Geometrical Structure of the Gold–Iron(III) Oxide Interfacial Perimeter for CO Oxidation. *Angewandte Chemie* **2018**, *130* (35), 11459–11463. https://doi.org/10.1002/ange.201805975.

(6) Zhao, K.; Tang, H.; Qiao, B.; Li, L.; Wang, J. High Activity of Au/γ-Fe2o3 for Co Oxidation: Effect of Support Crystal Phase in Catalyst Design. *ACS Catal* **2015**, *5* (6), 3528–3539. https://doi.org/10.1021/cs5020496.

(7) Li, L.; Wang, A.; Qiao, B.; Lin, J.; Huang, Y.; Wang, X.; Zhang, T. Origin of the High Activity of Au/FeOx for Low-Temperature CO Oxidation: Direct Evidence for a Redox Mechanism. *J Catal* **2013**, *299*, 90–100. https://doi.org/10.1016/j.jcat.2012.11.019.

(8) Zhang, Y.; Liu, J. X.; Qian, K.; Jia, A.; Li, D.; Shi, L.; Hu, J.; Zhu, J.; Huang, W. Structure Sensitivity of Au-TiO2 Strong Metal–Support Interactions. *Angewandte Chemie - International Edition* **2021**, *60* (21), 12074–12081. https://doi.org/10.1002/anie.202101928.

(9) Daniells, S. T.; Overweg, A. R.; Makkee, M.; Moulijn, J. A. The Mechanism of Low-Temperature CO Oxidation with Au/Fe2O 3 Catalysts: A Combined Mössbauer, FT-IR, and TAP Reactor Study. *J Catal* **2005**, *230* (1), 52–65. https://doi.org/10.1016/j.jcat.2004.11.020.

(10) Daniells, S. T.; Makkee, M.; Moulijn, J. A. The Effect of High-Temperature Pre-Treatment and Water on the Low Temperature CO Oxidation with Au/Fe2O3 Catalysts. *Catal Letters* **2005**, *100* (1–2), 39–47. https://doi.org/10.1007/s10562-004-3083-z.

(11) Klyushin, A. Y.; Jones, T. E.; Lunkenbein, T.; Kube, P.; Li, X.; Hävecker, M.; Knop-Gericke, A.; Schlögl, R. Strong Metal Support Interaction as a Key Factor of Au Activation in CO Oxidation. *ChemCatChem* **2018**, *10* (18), 3985–3989. https://doi.org/10.1002/cctc.201800972.

(12) Saavedra, J.; Pursell, C. J.; Chandler, B. D. CO Oxidation Kinetics over Au/TiO2 and Au/Al2O3 Catalysts: Evidence for a Common Water-Assisted Mechanism. *J Am Chem Soc* **2018**, *140* (10), 3712–3723. https://doi.org/10.1021/jacs.7b12758.

(13) Ojeda, M.; Zhan, B. Z.; Iglesia, E. Mechanistic Interpretation of CO Oxidation Turnover Rates on Supported Au Clusters. *J Catal* **2012**, *285* (1), 92–102. https://doi.org/10.1016/j.jcat.2011.09.015.

(14) Saavedra, J.; Doan, H. A.; Pursell, C. J.; Grabow, L. C.; Chandler, B. D. The Critical Role of Water at the Gold-Titania Interface in Catalytic CO Oxidation. *Science (1979)* **2014**, *345* (6204), 1599–1602. https://doi.org/10.1126/science.1256018.

(15) Jin, C.; Zhou, Y.; Han, S.; Shen, W. Water-Assisted Low-Temperature Oxidation of CO at the Au-Fe2O3Interface. *Journal of Physical Chemistry C* **2021**, *125* (47), 26031–26038. https://doi.org/10.1021/acs.jpcc.1c07995.

(16) Bongiorno, A.; Landman, U. Water-Enhanced Catalysis of CO Oxidation on Free and Supported Gold Nanoclusters. *Phys Rev Lett* **2005**, *95* (10), 1–4. https://doi.org/10.1103/PhysRevLett.95.106102.

(17) Daté, M.; Okumura, M.; Tsubota, S.; Haruta, M. Vital Role of Moisture in the Catalytic Activity of Supported Gold Nanoparticles. *Angewandte Chemie* **2004**, *116* (16), 2181–2184. https://doi.org/10.1002/ange.200453796.

(18) Kung, H. H.; Kung, M. C.; Costello, C. K. Supported Au Catalysts for Low Temperature CO Oxidation. *J Catal* **2003**, *216* (1–2), 425–432. https://doi.org/10.1016/S0021-9517(02)00111-2.

(19) Wang, Y. G.; Cantu, D. C.; Lee, M. S.; Li, J.; Glezakou, V. A.; Rousseau, R. CO Oxidation on Au/TiO2: Condition-Dependent Active Sites and Mechanistic Pathways. *J Am Chem Soc* **2016**, *138* (33), 10467–10476. https://doi.org/10.1021/jacs.6b04187.

(20) Fujitani, T.; Nakamura, I.; Takahashi, A. H2O Dissociation at the Perimeter Interface between Gold Nanoparticles and TiO2 Is Crucial for Oxidation of CO. *ACS Catal* **2020**, *10* (4), 2517–2521. https://doi.org/10.1021/acscatal.9b05195.

(21) Low Temperature Oxidation of Co over Gold Supported on Tio2 Fe2o3 and Co3o4.

(22) Carley, A. F.; Morgan, D. J.; Song, N.; Roberts, M. W.; Taylor, S. H.; Bartley, J. K.; Willock, D. J.; Howard, K. L.; Hutchings, G. J. CO Bond Cleavage on Supported Nano-Gold during Low Temperature Oxidation. *Physical Chemistry Chemical Physics* **2011**, *13* (7), 2528–2538. https://doi.org/10.1039/c0cp01852j.

(23) Daté, M.; Haruta, M. Moisture Effect on CO Oxidation over Au/TiO2 Catalyst. *J Catal* **2001**, *201* (2), 221–224. https://doi.org/10.1006/jcat.2001.3254.

(24) Li, L.; Wang, A.; Qiao, B.; Lin, J.; Huang, Y.; Wang, X.; Zhang, T. Origin of the High Activity of Au/FeOx for Low-Temperature CO Oxidation: Direct Evidence for a Redox Mechanism. *J Catal* **2013**, *299*, 90–100. https://doi.org/10.1016/j.jcat.2012.11.019.

(25) Zhang, Y.; Liu, J. X.; Qian, K.; Jia, A.; Li, D.; Shi, L.; Hu, J.; Zhu, J.; Huang, W. Structure Sensitivity of Au-TiO2 Strong Metal–Support Interactions. *Angewandte Chemie - International Edition* **2021**, *60* (21), 12074–12081. https://doi.org/10.1002/anie.202101928.

(26) Klyushin, A. Y.; Jones, T. E.; Lunkenbein, T.; Kube, P.; Li, X.; Hävecker, M.; Knop-Gericke, A.; Schlögl, R. Strong Metal Support Interaction as a Key Factor of Au Activation in CO Oxidation. *ChemCatChem* **2018**, *10* (18), 3985–3989. https://doi.org/10.1002/cctc.201800972.

(27) Tripathi, A. K.; Kamble, V. S.; Gupta, N. M. Microcalorimetry, Adsorption, and Reaction Studies of CO, O 2 , and CO + O 2 over Au/Fe 2 O 3 , Fe 2 O 3 , and Polycrystalline Gold Catalysts. *J Catal* **1999**, *187*, 332–342.

(28) Carabineiro, S. A. C.; Bogdanchikova, N.; Tavares, P. B.; Figueiredo, J. L. Nanostructured Iron Oxide Catalysts with Gold for the Oxidation of Carbon Monoxide. *RSC Adv* **2012**, *2* (7), 2957–2965. https://doi.org/10.1039/c2ra00724j.

(29) Guczi, L.; Horváth, D.; Pászti, Z.; Petõ, G. Effect of Treatments on Gold Nanoparticles: Relation between Morphology, Electron Structure and Catalytic Activity in CO Oxidation. *Catal Today* **2002**, *72* (1–2), 101–105. https://doi.org/10.1016/S0920-5861(01)00483-7.

(30) Khoudiakov, M.; Gupta, M. C.; Deevi, S. Au/Fe2O3 Nanocatalysts for CO Oxidation: A Comparative Study of Deposition-Precipitation and Coprecipitation Techniques. *Appl Catal A Gen* **2005**, *291* (1–2), 151–161. https://doi.org/10.1016/j.apcata.2005.01.042.

(31) Akita, T.; Maeda, Y.; Kohyama, M. Low-Temperature CO Oxidation Properties and TEM/STEM Observation of Au/γ-Fe2O3 Catalysts. *J Catal* **2015**, *324*, 127–132. https://doi.org/10.1016/j.jcat.2015.02.006.

(32) Šmit, G.; Strukan, N.; Crajé, M. W. J.; Lázár, K. A Comparative Study of CO Adsorption and Oxidation on Au/Fe2O3 Catalysts by FT-IR and in Situ DRIFTS Spectroscopies. *J Mol Catal A Chem* **2006**, *252* (1–2), 163–170. https://doi.org/10.1016/j.molcata.2006.02.058.

(33) Zhao, K.; Qiao, B.; Wang, J.; Zhang, Y.; Zhang, T. A Highly Active and Sintering-Resistant Au/FeOx-Hydroxyapatite Catalyst for CO Oxidation. *Chemical Communications* **2011**, *47* (6), 1779–1781. https://doi.org/10.1039/c0cc04171h.

(34) Holm, A.; Goodman, E. D.; Stenlid, J. H.; Aitbekova, A.; Zelaya, R.; Diroll, B. T.; Johnston-Peck, A. C.; Kao, K. C.; Frank, C. W.; Pettersson, L. G. M.; Cargnello, M. Nanoscale Spatial Distribution of Supported Nanoparticles Controls Activity and Stability in Powder Catalysts for CO Oxidation and Photocatalytic H2Evolution. *J Am Chem Soc* **2020**, *142* (34), 14481–14494. https://doi.org/10.1021/jacs.0c03842.

(35) Wang, C.; Gu, X. K.; Yan, H.; Lin, Y.; Li, J.; Liu, D.; Li, W. X.; Lu, J. Water-Mediated Mars-Van Krevelen Mechanism for CO Oxidation on Ceria-Supported Single-Atom Pt1 Catalyst. *ACS Catal* **2017**, *7* (1), 887–891. https://doi.org/10.1021/acscatal.6b02685.

(36) Baltrusaitis, J.; Schuttlefield, J. D.; Zeitler, E.; Jensen, J. H.; Grassian, V. H. Surface Reactions of Carbon Dioxide at the Adsorbed Water-Oxide Interface. *Journal of Physical Chemistry C* **2007**, *111* (40), 14870–14880. https://doi.org/10.1021/jp074677l.

(37) Schubert, M. M.; Hackenberg, S.; van Veen, A. C.; Muhler, M.; Plzak, V.; Behm, R. J. CO Oxidation over Supported Gold Catalysts -"Inert" and “Active” Support Materials and Their Role for the Oxygen Supply during Reaction. *J Catal* **2001**, *197* (1), 113–122. https://doi.org/10.1006/jcat.2000.3069.

(38) Kahlich, M. J.; Gasteiger, H. A.; Behm, R. J. *Kinetics of the Selective Low-Temperature Oxidation of CO in H 2-Rich Gas over Au/α-Fe 2 O 3*; 1999; Vol. 182. http://www.idealibrary.comon.

(39) Haruta, M. *Gold as a Novel Catalyst in the 21st Century: Preparation, Working Mechanism and Applications*.

(40) Han, Q.; Zhang, D.; Guo, J.; Zhu, B.; Huang, W.; Zhang, S. Improved Catalytic Performance of Au/α-Fe2O3-like-Worm Catalyst for Low Temperature CO Oxidation. *Nanomaterials* **2019**, *9* (8). https://doi.org/10.3390/nano9081118.